



Published in final edited form as:

AJNR Am J Neuroradiol. 2019 September ; 40(9): 1438–1444. doi:10.3174/ajnr.A6146.

Altered Relationship Between Working Memory And Brain Microstructure After Mild Traumatic Brain Injury

Sohae Chung, Ph.D.^{1,2,*}, Xiuyuan Wang, M.S.^{1,2}, Els Fieremans, Ph.D.^{1,2}, Joseph F. Rath, Ph.D.³, Prin Amorapanth, M.D.³, Farg-Yang A. Foo, M.D.⁴, Charles J. Morton, B.S.^{1,2}, Dmitry S. Novikov, Ph.D.^{1,2}, Steven R. Flanagan, M.D.³, Yvonne W. Lui, M.D.^{1,2}

¹Center for Advanced Imaging Innovation and Research (CAI2R), Department of Radiology, New York University School of Medicine, New York, NY

²Bernard and Irene Schwartz Center for Biomedical Imaging, Department of Radiology, New York University School of Medicine, New York, NY

³Department of Rehabilitation Medicine, New York University School of Medicine, New York, NY 10016, USA

⁴Department of Neurology, New York University Langone Health, New York, NY 10016, USA

Abstract

Background and Purpose: Working memory impairment is one of the most troubling and persistent symptoms after mild traumatic brain injury (MTBI). Here we investigate how working memory deficits relate to detectable WM microstructural injuries in order to discover robust biomarkers that allow for early identification of MTBI patients at highest risk of working memory impairments.

Materials and Methods: Diffusion MRI was performed on a 3T scanner with 5 b-values. Diffusion metrics of fractional anisotropy (FA), diffusivity and kurtosis (mean, radial, axial) as well as WM tract integrity (WMTI) were calculated. Auditory-verbal working memory was assessed using WAIS-IV subtests: 1) Digit Span (DS) including Forward (DSF), Backward (DSB) and Sequencing (DSS), and 2) Letter-Number Sequencing (LNS). We studied 19 MTBI patients within 4 weeks of injury and 20 normal controls (NC). Tract-based spatial statistics (TBSS) and ROI analyses were performed to reveal possible correlations between diffusion metrics and working memory performance with age and sex as covariates.

Results: ROI analysis found a significant positive correlation between axial kurtosis (AK) and DSB in MTBI (Pearson's $r=0.69$, corrected $p=0.04$), mainly present in the right superior longitudinal fasciculus that was not observed in NC. MTBI patients also appear to lose the normal associations typically seen in FA and axonal water fraction (AWF) with LNS. TBSS results also support our findings.

*Corresponding Author: Sohae Chung, PhD, 660 1st ave, 4th floor, New York, NY10016, USA, (Tel) 1-212-263-3324, sohae.chung@nyulangone.org.

Conclusion: Differences between MTBI and NC with regard to relationship between microstructure measures and working memory performance may relate to known axon perturbations occurring after injury.

INTRODUCTION

Mild traumatic brain injury (MTBI) is a significant public health problem with many serious consequences.^{1, 2} While the majority of MTBI patients recover symptomatically within 2–3 weeks after injury, at least 15% of patients report persistent cognitive complaints that are an important source of distress and disability after injury.^{3–5} Now an important body of work reveals MTBI-related WM injury using DTI^{6–8} and diffusion kurtosis imaging (DKI).^{9, 10} More recently, WM tract integrity (WMTI) metrics derived from an advanced compartmental diffusion WM model¹¹ have been proposed to describe microstructural characteristics in the intra- and extra-axonal environments of WM, including axonal water fraction (AWF), intra-axonal diffusivity (D_{axon}), extra-axonal axial ($D_{e,\parallel}$) and radial ($D_{e,\perp}$) diffusivities.

One of major barriers to applying such findings to clinical cohorts is that the disorder is extremely heterogenous and most current studies group clinically heterogenous cohorts of MTBI patients together representing a broad spectrum of clinical symptoms. Thus, there is a specific need to understand domain-specific symptoms as they relate to detectable microstructural injuries, in order to better understand patient specific injury and recovery.

One of the most common and clinically significant complaints in MTBI patients is deficits in working memory,^{3, 4, 12–15} which often negatively affect quality of life.¹⁶ This comes as no surprise as working memory, which involves the capacity to temporarily store and manipulate information in pursuit of a goal, is at the core of critical cognitive functions such as comprehension, learning, reasoning, and decision making.¹⁷ Working memory is conceptualized as comprising three main components: the central executive, responsible for manipulation of information and allocation of attention and processing resources, and two maintenance systems, the phonological loop (verbal and auditory information) and the visuospatial sketchpad (visual and spatial information).^{18–20} There have been a few studies showing associations of working memory performance with measures of WM microstructure such as fractional anisotropy (FA)²¹ and AWF^{22–24} in healthy individuals, believed to relate to differences in axon volume and myelination. However, such associations have not yet been investigated in MTBI patients.

Here, we hypothesize that WM injury in MTBI patients can affect the relationship between microstructural changes to the WM and working memory performance. To test this hypothesis, we investigate the relationship between WM microstructural changes assessed by using diffusion MRI (DTI, DKI, WMTI) and a set of Wechsler Adult Intelligence Scale-Fourth Edition (WAIS-IV)²⁵ subtests tapping auditory-verbal working memory functions in MTBI patients, comparing them against healthy controls. We also perform subgroup analyses based on working memory performance and time-since-injury.

MATERIALS AND METHODS

Study Population

This study has been approved by our Institutional Review Board. All experiments were performed in accordance with relevant guidelines and regulation, and written informed consents were provided by all subjects before the procedure. We prospectively recruited subjects who were seen for clinical care in the Emergency Department or Institutional Concussion Center. Inclusion criteria are: 1) adult individuals in the age range of 18 – 65 years, 2) diagnostic MTBI criteria defined by the American Congress of Rehabilitation Medicine (ACRM)²⁶ including either loss of consciousness of < 30 minutes or altered consciousness at time of accident and a Glasgow Coma Scale (GSC) of 13 – 15, and 3) injury within 4 weeks. We excluded patients with: 1) previous history of TBI, neurological illness or psychiatric disorder, 2) history of participation in organized contact sports, and 3) any contraindication to MRI. We also further excluded non-native English speakers and non-right-handed individuals in order to avoid any potential confounding effects of language and handedness. We studied 19 patients with MTBI (mean age, 30 ± 7 , age range, 22 – 45 years old; average time since injury, 16 days; 9 male) and 20 normal controls (NC) (mean age, 33 ± 10 , age range, 19 – 65 years old; 9 male). For all subjects, formal neurocognitive tests including WAIS-IV working memory subtests were performed and MR images were acquired within 1 day of neurocognitive tests. Additionally, to characterize subjects, Wide Range Achievement Test-4th Edition Word Reading subtest (WRAT-4) was performed and the scores were converted to IQ scores as a brief measure of intelligence. Subgroups of the subjects in this study were previously included in two works with non-overlapping hypotheses.^{24, 27}

MRI Protocol

MRI was performed using a 3T MR scanner (Skyra, Siemens Medical Solutions, Erlangen, Germany). Diffusion imaging was performed with 5 b-values (250, 1000, 1500, 2000, 2500 s/mm^2) using 5 diffusion encoding direction scheme (6, 20, 20, 30, 60, respectively). Three images with $b = 0 \text{ s/mm}^2$ were also acquired. Multiband (factor of 2)²⁸ EPI was used for accelerated acquisitions with anterior-posterior (AP) phase encoding direction. Other parameters included: field of view = 220 mm \times 220 mm, acquisition matrix = 88 \times 88, number of slices = 56, image resolution = 2.5 \times 2.5 \times 2.5 mm^3 , TR/TE = 4900/95 ms, bandwidth = 2104 Hz/pixel, a generalized autocalibrating partially parallel acquisitions (GRAPPA) factor of 2. An additional image with $b = 0 \text{ s/mm}^2$ with reversed phase encoding direction was acquired for geometric artifact correction. The total scan time was 12 minutes.

Working Memory Assessment

Working memory was assessed with age-appropriate WAIS-IV subtests,²⁵ which included Digit Span (DS) and Letter-Number Sequencing (LNS). In the DS Forward (DSF) task, examinees repeat a sequence of numbers read to them. In the DS Backward (DSB), the same procedure is followed, except that examinees repeat the numbers in reverse order, and in the DS Sequencing (DSS), examinees repeat the numbers in ascending order. In the Letter-Number Sequencing (LNS) task, examinees separate numbers from letters and state in ascending/alphabetical order a mixed sequence of numbers and letters read to them. Raw

scores were converted into standardized age-corrected z-scores with a zero mean and a unitary variation²⁵ with higher scores indicating better performance.

Image Analyses

Diffusion Image Processing—The diffusion images underwent the pre-processing steps including Marchenko-Pastur principal component analysis (MP-PCA) denoising,²⁹ Gibbs correction,³⁰ distortion correction with FSL's topup command, eddy current distortion and motion correction with FSL's eddy command, and outlier detection.³¹ Total 11 diffusion metrics including DTI (FA, mean diffusivity [MD], axial diffusivity [AD], radial diffusivity [RD]), DKI (mean kurtosis [MK], axial kurtosis [AK], radial kurtosis [RK]) and WMTI (AWF, D_{axon} , $D_{e,\parallel}$, $D_{e,\perp}$) metrics were calculated by using in-house software developed in MATLAB R2017a (The Mathworks, Inc., Natick, MA).

Tract-Based Spatial Statistics (TBSS)—We used the standard tract-based spatial statistics (TBSS)³² to reveal possible correlations between working memory test z-scores and diffusion metrics. Briefly, subject FA maps were normalized to the FA template through a nonlinear co-registration, and voxel-wise statistical analysis was performed on FA values projected onto the FA skeleton by looking for local maximum values perpendicular to the skeleton using a permutation-based nonparametric testing (FSL's randomize command) with the threshold free cluster enhancement (TFCE) option. All other parametric maps underwent the same transformations and processes. The tract skeleton was thresholded at FA of 0.2 for DTI and DKI metrics. For WMTI metrics, analysis was restricted to WM regions consisting of single-fiber orientations (FA threshold of 0.4), as recommended.^{11, 33} Age and sex were included as covariates. The number of permutations was set to 5000.

ROI Analysis—ROI analysis was performed on 18 major WM tracts, including genu/body/splenium of corpus callosum (gCC/bCC/sCC), right and left anterior/posterior limb of internal capsule (LIC), right and left anterior/superior/posterior corona radiata (aCR/sCR/pCR), right and left cingulum, right and left superior longitudinal fasciculus (SLF), and whole WM. ROI regions were generated based on the John Hopkins University (JHU) ICBM-DTI-81 WM labels atlas.³⁴ Briefly, all subjects FA maps were nonlinearly registered to the FA template and then a 'reversed warping' procedure was performed to assign the atlas labels to each subject's space. The ROIs in each subject space were manually corrected if necessary. For each ROI, mean value was obtained only in voxels with FA \geq 0.2 for DTI and DKI metrics and with FA \geq 0.4 for WMTI metrics, in order to restrict analysis to WM regions, as recommended.^{11, 33}

Statistical Analysis

MANCOVA was used to test group differences of length of education and WRAT-4 IQ scores, with age and sex as covariates, by using SPSS Statistics software version 25.0 (SPSS Inc, Chicago, Illinois). Results were considered significant for $p < 0.05$.

For TBSS, statistical threshold level of $p < 0.05$ was applied after family-wise error (FWE) correction for multiple comparisons.

For ROI analysis, both Pearson's partial correlation and Spearman rank correlation were performed to measure the associations between diffusion metrics and WAIS-IV subtest scores in each ROI, using SPSS. Age and sex were included as covariates. All p-values were corrected for multiple comparisons using Benjamini-Hochberg correction. Statistical threshold level of corrected $p < 0.05$ was used. Correlation coefficients (R) were calculated. We also used Fisher's R-to-Z transformation³⁵ to test for differences in between-group correlations.

Based on the ROI analysis results, specific regions demonstrating significant correlations with working memory performance were further interrogated by dividing subjects into subgroups based on their working memory test z-score (< 1 , ≥ 1) and time-since-injury (< 2 weeks, 2–4 weeks). Subgroup comparisons were done using MANCOVA with age as covariate. Results were considered significant for $p < 0.05$.

RESULTS

Average length of education for MTBI patients was 15.5 ± 1.7 years, not statistically different from healthy controls (16.3 ± 1.8 years). Also, WRAT-4 IQ scores were not statistically different between MTBI (108.5 ± 12.0) and NC (113.6 ± 14.3) groups. WAIS-IV subtests were not significantly correlated with age and length of education for MTBI and NC groups, except positive correlations between length of education and DSS in NC ($p = 0.03$).

From TBSS analysis, in the MTBI group, we found a significant positive correlation between AK and DSB primarily in the right SLF (Fig. 1(a)), that was not present in the NC group (Fig. 1(b)). Interestingly, we found complete loss of relationships between FA and LNS in the MTBI group (Fig. 2(a)), while a significant correlation was shown in the NC group (Fig. 2(b)), most notably in parietal WM, sCR/pCR, bCC/sCC, and SLF. We also found no significant correlation between AWF and LNS in the MTBI group (Fig. 3(a)), while there were multiple areas showing a statistically significant positive correlation between AWF and LNS, involving parietal WM, sCR/pCR and bCC/sCC (Fig. 3(b)). No other diffusion metrics showed area of significant correlation surviving correction for multiple comparisons.

ROI analysis also found a significant correlation between AK and DSB in the right SLF in the MTBI group (Pearson's $R = 0.69$, $p = 0.002$; Spearman's $Rho = 0.75$, $p = 0.0005$), that was not present in the NC group. The correlation coefficients observed in the MTBI and NC groups were significantly different (Fisher R-to-Z transformation, $p = 0.01$). On the other hand, we also observed loss of relationships between FA and LNS in the MTBI group, but found a significant positive correlation in the right pCR in the NC group (Pearson's $R = 0.67$, $p = 0.002$; Spearman's $Rho = 0.57$, $p = 0.014$). The correlation coefficients observed in the MTBI and NC groups were not significantly different, but there was a trend towards significance (Fisher R-to-Z transformation, $p = 0.06$). No other significant correlations were found after correction for multiple comparisons. These results are summarized in Table 1.

Based on the results of the ROI analysis, subjects were further divided into subgroups according to their working memory test z-scores (< 1 or ≥ 1) and time-since-injury (< 2

weeks or 2–4 weeks). Details of the subgroup characteristics are given in Table 2. With regard to subgroup analysis, we found a significant difference in AK between the MTBI subgroup of 2–4 weeks of injury with $DSB < 1$ and the MTBI subgroup of 2–4 weeks of injury with $DSB \geq 1$ within the right SLF (Fig. 4(a)). Significant differences in FA were shown between the MTBI subgroup of < 2 weeks of injury with $LNS < 1$ and the NC subgroup with $LNS < 1$, and between the NC subgroup with $LNS < 1$ and the NC subgroup with $LNS \geq 1$, within the right pCR (Fig. 4(b)).

DISCUSSION

This study shows significant differences in the relationships between specific WM microstructural markers and auditory-verbal working memory performance between MTBI patients and healthy controls. Specifically, in the MTBI group, a significant correlation between AK and DSB was present in the right SLF, while the NC group demonstrated no such relationship (Fig. 1), a finding observed using both TBSS and ROI analyses. MTBI patients also appear to lose the normal associations seen in controls between diffusion metrics (FA, AWF) and LNS (Figs. 2, 3). Furthermore, subgroup analyses also showed a significant difference of AK between the MTBI subgroup of 2–4 weeks of injury with $DSB < 1$ and the MTBI subgroup of 2–4 weeks of injury with $DSB \geq 1$. A significant difference was also found between the MTBI subgroup of < 2 weeks of injury and the NC subgroup, both having $LNS < 1$.

Notably, the relationship between AK and DSB in MTBI subjects is mainly present in the right SLF (Fig. 1), a structure critical for attention, memory, emotion and language,^{36, 37} linking fronto-parietal WM regions critical to working memory.^{38–40} In particular, the right SLF is critical for attention,⁴¹ visuospatial function,⁴² and short-term memory.⁴³ Previously, similar results were reported showing relations between the SLF and working memory deficits assessed by FA and visual 2-back d-prime index in severe and diffuse TBI patients.⁴⁴ In this study, we found decreased AK in the right SLF, reflecting decreased tissue complexity along the long axis of the axon⁴⁵ in MTBI patients with poorer performance on DSB. AK is known from animal validation studies to be affected by axon injury⁴⁶ as well as secondary reactive astrogliosis.⁴⁷

Also differentiating MTBI from NC groups, in TBSS analysis, was a loss of diffusely present normal associations that we have seen in healthy controls (Figs. 2, 3); in controls, it has been shown that FA and AWF directly correlate with performance on LNS, a complex working memory task.²⁴ However, in MTBI patients we found a disruption in this normal relationship, presumed to relate to WM injuries known to occur after MTBI,¹⁴ as AWF is a measure that reflects axon density and/or myelination.

ROI analyses (Table 1) showed related statistically significant correlations focused in the right SLF in MTBI patients as well as in the right pCR in healthy controls, compared with the more diffuse TBSS results. TBSS uses maximum values projected onto the WM skeleton, making it more sensitive to maximal deviations in diffusion metrics. Both TBSS and ROI analyses reveal positive correlations in the right SLF and right pCR, suggesting these regions to be strong, potential anatomical landmarks important to working memory

performance, and possibly impairment. Along with the SLF, a structure critical to working memory,^{38–40} the CR is also a complex bundle of fibers related to working memory since it consists of several separate pathways connecting cerebral cortex to subcortical structures^{24, 48, 49} including fiber tracts in the pCR which connect to the precuneus, a part of the default-mode network implicating in working memory performance.^{50, 51}

With regard to the subgroup analysis, within the same time-since-injury period of 2–4 weeks, there was a significant difference in AK between the MTBI subgroups with higher and lower working memory performance in the right SLF (Fig. 4(a)). Decreased AK, believed to relate to axonal injury⁴⁶ and/or secondary reactive astrogliosis⁴⁷, may specifically be more a useful indicator in the MTBI subgroup with lower working memory performance. Also, within the lower LNS range, significantly elevated FA was observed in the MTBI subgroup within 2 weeks of injury compared to corresponding the NC subgroup with the same lower LNS range (Fig. 4(b)). Elevated FA reported frequently within 2 weeks of injury, believed to reflect injury-related cytotoxic edema⁵² or reactive astrogliosis⁵³. We only found a significant difference in FA between the MTBI subgroup within 2 weeks of injury and the NC subgroup, only in the lower LNS range, not in the higher LNS range, suggesting that understanding the relationships between domain-specific symptoms, such as working memory deficits, and underlying microstructural injuries is important for patient management (e.g., pharmacological intervention to inhibit inflammation and reduce the neurotoxic effects of reactive gliosis).

There are several limitations in the presented study. First, there is a wide age ranges from 19 – 65 years. Any age effects were minimized by using age-corrected WAIS-IV subtest z-scores derived from the published normative sample (n = 2200) divided into 13 age bands, spanning ages 16 to 90.²⁵ Moreover, age is included as a covariate in all statistical analyses. Second, subgroups were defined based on a somewhat arbitrary statistical threshold value for LNS and DSB (Fig. 4). Further work could be done to study various performance groups. Third, this study includes a relatively small number of total subjects and point toward the need for larger studies of working memory dysfunction and brain injury in patients with MTBI. Fourth, this study did not examine the underlying processes that contribute to working memory tasks such as DS and LNS. Further work could be done to focus on component processes such as attention and maintenance of information. Furthermore, as mentioned previously, TBSS uses maximum values projected onto the WM skeleton along an orthogonal line, making it more sensitive to maximal deviations in diffusion metrics, but also reducing the need for image smoothing and alleviating any residual misalignment.⁵⁴ In this study, we use both TBSS and ROI approaches to rigorously assess both diffuse and regional WM.

CONCLUSIONS

There are differences between MTBI patients within 4 weeks of injury and healthy controls in terms of the relationships between brain microstructure and working memory performance. These findings may relate to known WM injury and changes in functional organization occurring after MTBI. Further study on the effect of time-since-injury on

working memory performance may provide insight into the temporal dynamics of working memory deficits in MTBI patients.

Acknowledgements

This work was supported in part by grand funding from the National Institutes of Health (NIH): R01 NS039135–11 and R21 NS090349, National Institute for Neurological disorders and Stroke (NINDS). This work was also performed under the rubric of the Center for Advanced Imaging Innovation and Research (CAI²R, www.cai2r.net), a NIBIB Biomedical Technology Resource Center (NIH P41 EB017183).

Grant supports: NIH R01 NS039135–11, R21 NS090349, P41 EB017183

ABBREVIATIONS

AD	axial diffusivity
AK	axial kurtosis
AWF	axonal water fraction
CR	corona radiata
D_{axon}	intra-axonal diffusivity
D_{e,l}	extra-axonal axial diffusivity
D_{e,r}	extra-axonal radial diffusivity
DSF	digit span forward
DSB	digit span backward
DSS	digit span sequencing
FA	fractional anisotropy
LNS	letter-number sequencing
MD	mean diffusivity
MK	mean kurtosis
MTBI	mild traumatic brain injury
NC	normal control
RD	radial diffusivity
RK	radial kurtosis
SLF	superior longitudinal fasciculus
TBSS	tract-based spatial statistics
WMTI	white matter tract integrity

REFERENCES

1. Taylor CA, Bell JM, Breiding MJ, et al. Traumatic brain injury-related emergency department visits, hospitalizations, and deaths - United States, 2007 and 2013. *MMWR Surveill Summ* 2017;66:1–16
2. Centers for Disease Control and Prevention (CDC) National Center for Injury Prevention and Control. Report to congress on mild traumatic brain injury in the United States: steps to prevent a serious public health problem. Atlanta, GA, USA: Centers for Disease Control and Prevention; 2003
3. Roe C, Sveen U, Alvsaker K, et al. Post-concussion symptoms after mild traumatic brain injury: influence of demographic factors and injury severity in a 1-year cohort study. *Disabil Rehabil* 2009;31:1235–1243 [PubMed: 19116810]
4. Chen CJ, Wu CH, Liao YP, et al. Working memory in patients with mild traumatic brain injury: functional MR imaging analysis. *Radiology* 2012;264:844–851 [PubMed: 22829681]
5. Ruff R Two decades of advances in understanding of mild traumatic brain injury. *J Head Trauma Rehabil* 2005;20:5–18 [PubMed: 15668567]
6. Mayer AR, Ling J, Mannell MV, et al. A prospective diffusion tensor imaging study in mild traumatic brain injury. *Neurology* 2010;74:643–650 [PubMed: 20089939]
7. Niogi SN, Mukherjee P, Ghajar J, et al. Extent of microstructural white matter injury in postconcussive syndrome correlates with impaired cognitive reaction time: a 3T diffusion tensor imaging study of mild traumatic brain injury. *AJNR Am J Neuroradiol* 2008;29:967–973 [PubMed: 18272556]
8. Rutgers DR, Toulgoat F, Cazejust J, et al. White matter abnormalities in mild traumatic brain injury: a diffusion tensor imaging study. *AJNR Am J Neuroradiol* 2008;29:514–519 [PubMed: 18039754]
9. Stokum JA, Sours C, Zhuo J, et al. A longitudinal evaluation of diffusion kurtosis imaging in patients with mild traumatic brain injury. *Brain Inj* 2015;29:47–57 [PubMed: 25259786]
10. Grossman EJ, Jensen JH, Babb JS, et al. Cognitive impairment in mild traumatic brain injury: a longitudinal diffusional kurtosis and perfusion imaging study. *AJNR Am J Neuroradiol* 2013;34:951–957, S951–953 [PubMed: 23179649]
11. Fieremans E, Jensen JH, Helpert JA. White matter characterization with diffusional kurtosis imaging. *Neuroimage* 2011;58:177–188 [PubMed: 21699989]
12. Sandry J, Chiou KS, DeLuca J, et al. Individual differences in working memory capacity predicts responsiveness to memory rehabilitation after traumatic brain injury. *Arch Phys Med Rehabil* 2016;97:1026–1029 e1021 [PubMed: 26657213]
13. van der Horn HJ, Liemburg EJ, Scheenen ME, et al. Post-concussive complaints after mild traumatic brain injury associated with altered brain networks during working memory performance. *Brain Imaging Behav* 2016;10:1243–1253 [PubMed: 26667033]
14. McAllister TW, Flashman LA, McDonald BC, et al. Mechanisms of working memory dysfunction after mild and moderate TBI: evidence from functional MRI and neurogenetics. *J Neurotrauma* 2006;23:1450–1467 [PubMed: 17020482]
15. McDowell S, Whyte J, D'Esposito M. Working memory impairments in traumatic brain injury: evidence from a dual-task paradigm. *Neuropsychologia* 1997;35:1341–1353 [PubMed: 9347480]
16. Hoofien D, Gilboa A, Vakil E, et al. Traumatic brain injury (TBI) 10–20 years later: a comprehensive outcome study of psychiatric symptomatology, cognitive abilities and psychosocial functioning. *Brain Inj* 2001;15:189–209 [PubMed: 11260769]
17. Kayser AS, Ballard ME, D'Esposito M. Working memory and TBI In: Alloway TP, ed. *Clinical Developmental Disorders: Theories, Debates, and Interventions*. New York, NY: Routledge; 2018:180–195
18. Baddeley A Working memory: looking back and looking forward. *Nat Rev Neurosci* 2003;4:829–839 [PubMed: 14523382]
19. Baddeley A Working memory: theories, models, and controversies. *Annu Rev Psychol* 2012;63:1–29 [PubMed: 21961947]
20. Klauer KC, Zhao Z. Double dissociations in visual and spatial short-term memory. *J Exp Psychol Gen* 2004;133:355–381 [PubMed: 15355144]

21. Takeuchi H, Taki Y, Sassa Y, et al. Verbal working memory performance correlates with regional white matter structures in the frontoparietal regions. *Neuropsychologia* 2011;49:3466–3473 [PubMed: 21906608]
22. Golestani AM, Miles L, Babb J, et al. Constrained by our connections: white matter's key role in interindividual variability in visual working memory capacity. *J Neurosci* 2014;34:14913–14918 [PubMed: 25378158]
23. Lazar M Working memory: how important is white matter? *Neuroscientist* 2017;23:197–210 [PubMed: 30231842]
24. Chung S, Fieremans E, Kucukboyaci NE, et al. Working memory and brain tissue microstructure: white matter tract integrity based on multi-shell diffusion MRI. *Sci Rep* 2018;8:3175 [PubMed: 29453439]
25. Wechsler D Wechsler Adult Intelligence Scale. Pearson Assessment; 2008
26. Klonoff PS, Costa LD, Snow WG. Predictors and indicators of quality of life in patients with closed-head injury. *J Clin Exp Neuropsychol* 1986;8:469–485 [PubMed: 3805248]
27. Chung S, Fieremans E, Wang X, et al. White matter tract integrity: an indicator of axonal pathology after mild traumatic brain injury. *J Neurotrauma* 2018;35:1015–1020 [PubMed: 29239261]
28. Setsompop K, Gagoski BA, Polimeni JR, et al. Blipped-controlled aliasing in parallel imaging for simultaneous multislice echo planar imaging with reduced g-factor penalty. *Magn Reson Med* 2012;67:1210–1224 [PubMed: 21858868]
29. Veraart J, Fieremans E, Novikov DS. Diffusion MRI noise mapping using random matrix theory. *Magn Reson Med* 2016;76:1582–1593 [PubMed: 26599599]
30. Kellner E, Dhital B, Kiselev VG, et al. Gibbs-ringing artifact removal based on local subvoxel-shifts. *Magn Reson Med* 2016;76:1574–1581 [PubMed: 26745823]
31. Collier Q, Veraart J, Jeurissen B, et al. Iterative reweighted linear least squares for accurate, fast, and robust estimation of diffusion magnetic resonance parameters. *Magn Reson Med* 2015;73:2174–2184 [PubMed: 24986440]
32. Smith SM, Jenkinson M, Johansen-Berg H, et al. Tract-based spatial statistics: voxelwise analysis of multi-subject diffusion data. *Neuroimage* 2006;31:1487–1505 [PubMed: 16624579]
33. Jensen JH, McKinnon ET, Glenn GR, et al. Evaluating kurtosis-based diffusion MRI tissue models for white matter with fiber ball imaging. *NMR Biomed* 2017;30
34. Mori S, Oishi K, Jiang H, et al. Stereotaxic white matter atlas based on diffusion tensor imaging in an ICBM template. *Neuroimage* 2008;40:570–582 [PubMed: 18255316]
35. Fisher RA. *Statistical methods for research workers*. Edinburgh, London: Oliver and Boyd; 1948
36. Mesulam MM. From sensation to cognition. *Brain* 1998;121 (Pt 6):1013–1052 [PubMed: 9648540]
37. Petrides M, Pandya DN. Comparative cytoarchitectonic analysis of the human and the macaque ventrolateral prefrontal cortex and corticocortical connection patterns in the monkey. *Eur J Neurosci* 2002;16:291–310 [PubMed: 12169111]
38. Cohen JD, Perlstein WM, Braver TS, et al. Temporal dynamics of brain activation during a working memory task. *Nature* 1997;386:604–608 [PubMed: 9121583]
39. Prabhakaran V, Narayanan K, Zhao Z, et al. Integration of diverse information in working memory within the frontal lobe. *Nat Neurosci* 2000;3:85–90 [PubMed: 10607400]
40. Todd JJ, Marois R. Capacity limit of visual short-term memory in human posterior parietal cortex. *Nature* 2004;428:751–754 [PubMed: 15085133]
41. Frye RE, Hasan K, Malmberg B, et al. Superior longitudinal fasciculus and cognitive dysfunction in adolescents born preterm and at term. *Dev Med Child Neurol* 2010;52:760–766 [PubMed: 20187879]
42. Hoefl F, Barnea-Goraly N, Haas BW, et al. More is not always better: increased fractional anisotropy of superior longitudinal fasciculus associated with poor visuospatial abilities in Williams syndrome. *J Neurosci* 2007;27:11960–11965 [PubMed: 17978036]
43. Chechlacz M, Gillebert CR, Vangkilde SA, et al. Structural variability within frontoparietal networks and individual differences in attentional functions: an approach using the theory of visual attention. *J Neurosci* 2015;35:10647–10658 [PubMed: 26224851]

44. Palacios EM, Fernandez-Espejo D, Junque C, et al. Diffusion tensor imaging differences relate to memory deficits in diffuse traumatic brain injury. *BMC Neurol* 2011;11:24 [PubMed: 21345223]
45. Jensen JH, Helpert JA. MRI quantification of non-Gaussian water diffusion by kurtosis analysis. *NMR Biomed* 2010;23:698–710 [PubMed: 20632416]
46. Andersson G, Oradd G, Sultan F, et al. In vivo diffusion tensor imaging, diffusion kurtosis imaging, and tractography of a sciatic nerve injury model in rat at 9.4T. *Sci Rep* 2018;8:12911 [PubMed: 30150697]
47. Zhuo J, Xu S, Proctor JL, et al. Diffusion kurtosis as an in vivo imaging marker for reactive astrogliosis in traumatic brain injury. *Neuroimage* 2012;59:467–477 [PubMed: 21835250]
48. Tang CY, Eaves EL, Ng JC, et al. Brain networks for working memory and factors of intelligence assessed in males and females with fMRI and DTI. *Intelligence* 2010;38:293–303
49. Long YC, Ouyang X, Liu ZN, et al. Associations among suicidal ideation, white matter integrity and cognitive deficit in first-episode schizophrenia. *Front Psychiatry* 2018;9
50. Esposito F, Aragri A, Latorre V, et al. Does the default-mode functional connectivity of the brain correlate with working-memory performances? *Arch Ital Biol* 2009;147:11–20 [PubMed: 19678593]
51. Bluhm RL, Clark CR, McFarlane AC, et al. Default network connectivity during a working memory task. *Human Brain Mapping* 2011;32:1029–1035 [PubMed: 20648663]
52. Shenton ME, Hamoda HM, Schneiderman JS, et al. A review of magnetic resonance imaging and diffusion tensor imaging findings in mild traumatic brain injury. *Brain Imaging Behav* 2012;6:137–192 [PubMed: 22438191]
53. Budde MD, Janes L, Gold E, et al. The contribution of gliosis to diffusion tensor anisotropy and tractography following traumatic brain injury: validation in the rat using Fourier analysis of stained tissue sections. *Brain* 2011;134:2248–2260 [PubMed: 21764818]
54. Bach M, Laun FB, Leemans A, et al. Methodological considerations on tract-based spatial statistics (TBSS). *Neuroimage* 2014;100:358–369 [PubMed: 24945661]

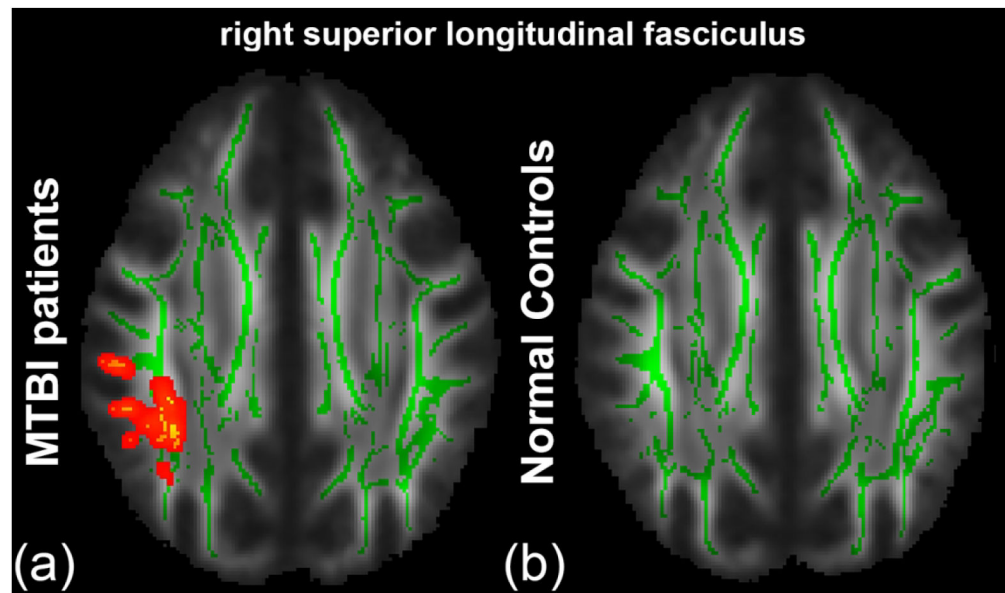


Figure 1.

TBSS results show a significant positive correlation between AK and DSB. Mean FA skeleton (green) overlaid on the mean FA map. Significantly correlated voxels (corrected $p < 0.05$) are shown in heat map overlay in the right SLF in (a) the MTBI group, but not seen in (b) the NC group.

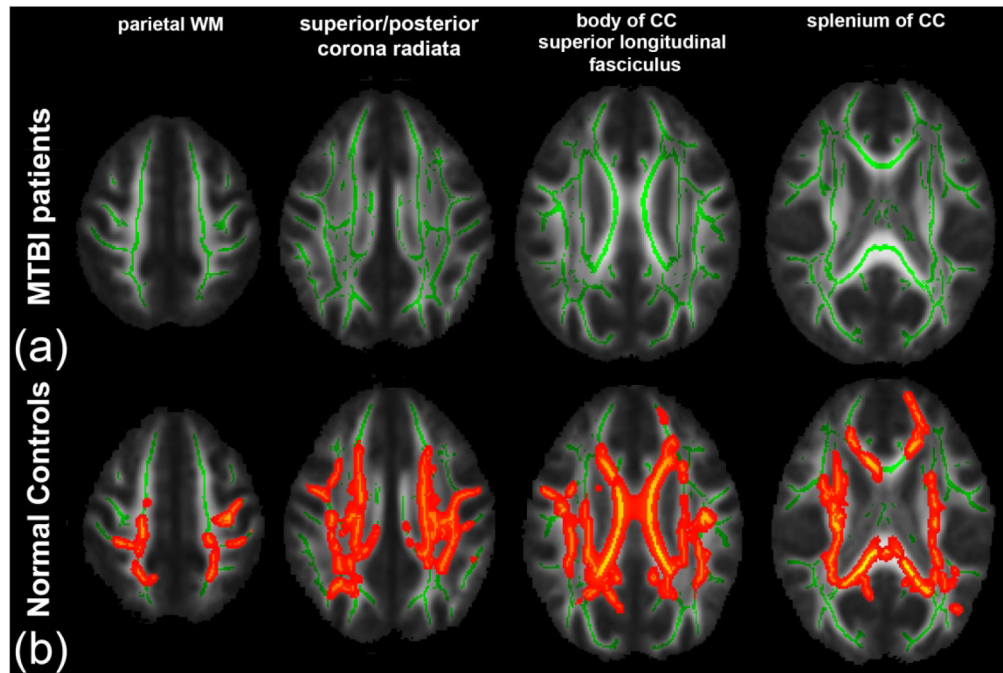


Figure 2.

TBSS results show a significant positive correlation between FA and LNS. Mean FA skeleton (green) overlaid on the mean FA map. Significantly correlated voxels (corrected $p < 0.05$) are shown in heat map overlay. (a) In the MTBI group, no correlation was found. (b) In the NC group, significantly correlated voxels involve parietal WM, sCR/pCR, bCC/sCC and SLF.

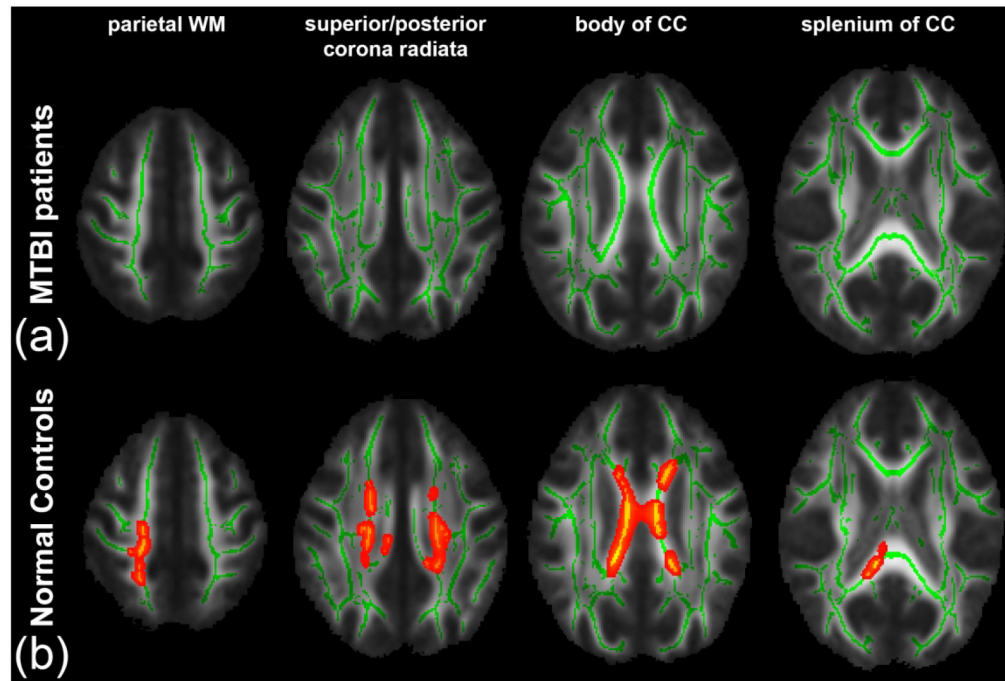


Figure 3.

TBSS results show a significant positive correlation between AWF and LNS. Mean FA skeleton (green) overlaid on the mean FA map. Significantly correlated voxels (corrected $p < 0.05$) are shown in heat map overlay. (a) In the MTBI group, no correlation was found. (b) In the NC group, significantly correlated voxels involve parietal WM, sCR/pCR and bCC/sCC.

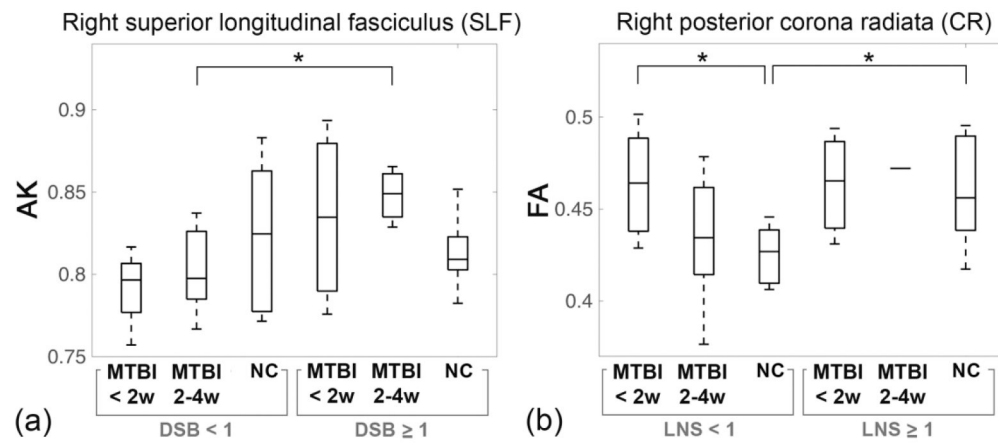


Figure 4.

Results of subgroup analysis. (a) Boxplots of AK show a significant difference between the MTBI subgroup of 2–4 weeks of injury with DSB < 1 and the MTBI subgroup of 2–4 weeks of injury with DSB ≥ 1. (b) Boxplots of FA show significant differences between the MTBI subgroup of < 2 weeks of injury with LNS < 1 and the NC subgroup with LNS < 1; and between the NC subgroup with LNS < 1 and the NC subgroup with LNS ≥ 1. *p < 0.05.

Table 1.

Results of the ROI analysis showing significant positive correlations between AK and DSB in the MTBI group, and between FA and LNS in the NC group. Corrected p-values (p*) after Benjamini-Hochberg correction for multiple comparison are presented. Significant results are highlighted in bold.

Diffusion Metrics vs Working Memory	ROI	MTBI				NC				Fisher's R-to-Z
		Pearson		Spearman		Pearson		Spearman		
		R	p*	Rho	p*	R	p*	Rho	p*	Z[p]
AK vs DSB	right SLF	0.69	0.04	0.75	0.01	0.04	1.20	0.11	1.48	2.32 [0.01]
FA vs LNS	right pCR	0.25	2.29	0.24	0.8	0.67	0.04	0.57	0.09	-1.59 [0.06]

Table 2.

Subgroup characteristics defined by their working memory test z-scores (LNS, DSB < 1 or 1) and time since injury (< 2 weeks or 2–4 weeks).

	LNS < 1			LNS 1		
	MTBI < 2 weeks	MTBI 2–4 weeks	NC	MTBI < 2 weeks	MTBI 2–4 weeks	NC
N	5	10	9	3	1	11
age	31 ± 6	31 ± 9	31 ± 8	25 ± 3	31	35 ± 12
LNS	-0.13 ± 0.51	0.07 ± 0.41	0.07 ± 0.32	1.55 ± 0.39	2	1.82 ± 0.62
	DSB < 1			DSB 1		
	MTBI < 2 weeks	MTBI 2–4 weeks	NC	MTBI < 2 weeks	MTBI 2–4 weeks	NC
N	4	7	12	4	4	8
age	30 ± 6	29 ± 8	31 ± 7	37 ± 8	26 ± 4	37 ± 14
DSB	-0.67 ± 0.27	-0.24 ± 0.25	0.08 ± 0.38	1.42 ± 0.5	1.58 ± 0.32	1.79 ± 0.71